NASA-CR-177175

P-50

IN-11060

ERTS

Naval Environmental Prediction Research Facility
Monterey, California 93940

FINAL REPORT

Contract NAG 5-289

Development of a Variational SEASAT Data Analysis Technique

by

Dr. Yoshi K. Sasaki
Dr. Lang-Ping Chang
Cooperative Institute for Mesoscale Meteorological Studies
The University of Oklahoma
Norman, OK 73019

QS473598

and

Dr. James S. Goerss
Naval Environmental Prediction Research Facility
Monterey, CA 93943

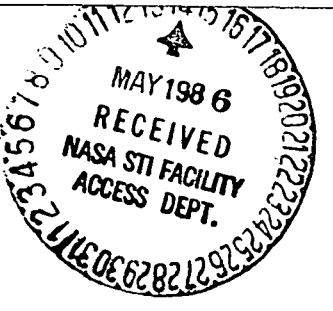
NQ449110

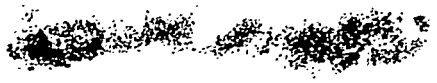
(NASA-CR-177175) DEVELOPMENT OF A VARIATIONAL SEASAT DATA ANALYSIS TECHNIQUE Final Report (Oklahoma Univ.) 50 p CSCL 05B

N86-31942

Unclas
G3/43 42902

April 1986





Development of a Variational SEASAT Data Analysis Technique

L. P. Chang
Y. K. Sasaki

Cooperative Institute for Mesoscale Meteorological Studies
The University of Oklahoma
Norman, OK 73019

and

J. S. Goerss

Naval Environmental Prediction Research Facility
Monterey, CA 93943

April 1986

ABSTRACT

Oceans are data-sparse areas in terms of conventional weather observations. The surface pressure field obtained solely by analyzing the conventional weather data is not expected to possess high accuracy. On the other hand, in entering asynoptic data such as satellite-derived temperature soundings into an atmospheric prediction system, an improved surface pressure analysis is crucial for obtaining more accurate weather predictions because the mass distribution of the entire atmosphere will be better represented in the system as a result of the more accurate surface pressure field. In order to obtain improved surface pressure analyses over the oceans, a variational adjustment technique was developed to help blend the densely distributed surface wind data derived from the SEASAT-A radar observations into the sparsely distributed conventional pressure data. A simple marine boundary layer scheme employed in the adjustment technique was discussed. In addition, a few aspects of the current technique were determined by numerical experiments.

TABLE OF CONTENTS

	PAGE
1. Introduction	1
2. Retrieval of the Sea Surface Wind from the SEASAT-A Satellite Observations	2
3. Variational SEASAT Data Analysis Technique	5
a. Estimate of the surface geostrophic wind	6
b. Variational adjustment technique	8
4. Results of Numerical Experiments	10
a. Determination of weights	10
b. Observational density and quality of pressure data	14
c. Effect of quality of SEASAT-derived wind data	18
d. Influence of surface temperature field	19
5. Concluding Remarks	20
Tables	24
Figure Captions	32
Figures	33
References	45

1. Introduction

Approximately 70% of the earth's surface is covered by oceans. In terms of conventional meteorological observations, oceans are data-sparse areas. With the development of weather satellites in the 1960's, a vast amount of remotely sensed asynoptic data has since become available over the ocean areas. Among various satellite weather data, temperature soundings are of great potential use in determining the mass distribution of the entire atmosphere for global scale models. The utility of the temperature soundings, however, crucially depends upon the quality of the sea-level pressure analysis. It thus follows that an improved sea-level pressure analysis in data-sparse areas over the oceans is vital for improved accuracy of the geopotential height information derived from the satellite soundings. This will, in turn, result in a better representation of the entire mass field in an atmospheric prediction system. Since the surface wind is closely associated with the surface pressure gradient, utilization of satellite-derived surface winds along with conventional weather data is expected to considerably improve the sea-level pressure analysis in the data-sparse ocean areas. The variational SEASAT data analysis technique is specifically designed for this purpose.

Stated in a brief manner, the working principle of the SEASAT-A satellite sensing of the surface wind is basically as follows: The microwave radar scatterometer carried by the SEASAT-A satellite is very sensitive to the backscatter of the centimeter length ocean waves created by the action of the surface wind over the oceans. As a result, one can derive the vector wind over the sea surface by analyzing the backscatter of the radar waves. Jones et al. (1982) compared the SEASAT-derived surface wind data with observations from the Joint Air Sea Interaction Experiment (JASIN) and concluded that the satellite-derived sea surface

wind has an accuracy of up to ±2 m/s in speed and ±20° in direction. These numbers will be considered characteristic of retrieved SEASAT wind fields. By combining the densely spaced SEASAT-derived wind data with the sparsely distributed sea surface pressure observations via a variational adjustment technique subject to some appropriate physical constraint(s), an improvement in the sea-level pressure analysis is expected. Such an improvement will certainly be very helpful in upgrading model forecasts of the atmospheric prediction systems.

In the following sections, we shall demonstrate how a simple marine boundary layer scheme in conjunction with a variational adjustment technique can be developed to help improve the sea-level pressure analysis by using SEASAT-derived wind in a limited-area domain in the ocean.

2. Retrieval of Sea Surface Wind from SEASAT-A Satellite Observations

The SEASAT-A satellite was launched on June 28, 1978 by the National Aeronautics and Space Administration. It was the first satellite dedicated to establishing the usefulness of microwave sensors for remote sensing of the oceans. After just a little more than three months of operation, it failed due to a massive short circuit in its electrical power system. In spite of its short operational life, valuable experimental data were collected.

One of the sensors aboard the SEASAT-A satellite was a radar scatterometer for detecting the surface winds over the ocean. The physical principle behind the wind detection lies in the sensitivity of the microwave radar backscatter to the centimeter length ocean waves created by the action of the surface wind. This is known as Bragg scattering (Wright, 1966; Moore and Fung, 1979). The strength of the radar backscattering cross section, σ^0, is proportional to the capillary wave amplitude which is assumed to be in equilibrium with the wind friction speed u_*. The wind direction can be determined because the radar backscatter is

anisotropic. Once the friction speed u_* is given, the wind at 19.5 m above the sea level under a neutral stability condition can be obtained. This wind is defined as the satellite-derived wind that would result if the atmosphere were neutrally stratified with a dry adiabatic lapse rate.

The history and details of the development of a geophysical algorithm to compute the 19.5 m neutral stability wind speed and direction from radar backscatter measurements are given by Jones et al. (1982). Three candidate algorithms were developed by researchers from the University of Kansas (Dome et al, 1977), the City University of New York (Pierson et al, 1974), and by the Remote Sensing System (Jones et al, 1978). A review of their work is given by Schroeder et al. (1982). The official wind vector algorithm known as SASS-I (SEASAT-A Satellite Scatterometer), described in Jones et al. (1982), represents a cooperative effort by the algorithm developers to incorporate the desirable features of its predecessors into a single algorithm.

The SASS-I model function is expressed by

$$F(\theta, x, \varepsilon, w) = \log_{10}\sigma^0 = G(\theta, x, \varepsilon) + H(\theta, x, \varepsilon) \log_{10} w \quad \ldots\ldots\ldots (2.1)$$

where w is the windspeed. The values of functions G and H are tabulated for incidence angles θ from 0° to 70°, for relative azimuth angle x (antenna azimuth minus wind direction) from 0° to 180°, and for horizontal and vertical polarization, ε= H or V. This lookup table, called the SASS-I Table, is given by Schroeder et al. (1982).

Given the model function, estimates of the wind speed, W, and direction, α, are found which produce local minima for the following sum of squares:

$$S(W, \alpha) = \sum_{i=1}^{N} \{\log_{10}\sigma_i^o - F(\theta_i, x_i, \varepsilon_i, W)\}^2/\delta_i^2 \quad \ldots\ldots\ldots\ldots\ldots\ldots (2.2)$$

where

$$x_i = \phi_i - \alpha.$$

The sum is over the N observations in a data group. The instrument parameters σ_i^o, θ_i, ϕ_i, and ε_i are the radar backscatter cross section, the incidence angle, the antenna azimuth angle, and the polarization for the i-th observation, respectively. The sum is weighted by $1/\delta_i^2$ where δ_i is the expected standard deviation between the σ^o measurement and the model function. Unfortunately, the number of candidate wind vectors (called aliases) varies from two to four (with four being most common). One alias will correspond to the solution for the true wind vector, and the others will be false solutions. Given that the proper alias has been determined, Jones et al. (1982) reported that comparisons of SASS-derived winds with high-quality independent analyses at the JASIN-SEASAT workshop show better agreement than the SASS specification of ± 2m/s for wind speed and ± 20° for wind direction.

Using a large-scale marine planetary boundary layer model (Brown and Liu, 1982), Brown et al. (1982) calculated synoptic scale wind fields for comparison with surface data collected during JASIN and the Gulf of Alaska Experiment (GOASEX). Observations of the synoptic-scale pressure and temperature fields served as input to the model in order to obtain the wind field. These analyses did not use satellite-derived wind observations. They found that the model-derived wind fields, when compared with the JASIN and GOASEX platform wind values, yielded a maximum error of only ± 2 m/s and ± 20°. This is only equal to the SASS

specification accuracies. Brown and Liu (1982) reported that at mid-latitudes, a 1 mb error in 400 km grid pressures would contribute 2 m/s error to a 10 m/s wind. The implication of this is that for a wind field with average speed above 10 m/s we may expect to obtain synoptic-scale pressure gradient information from satellite-derived surface wind measurements with reasonable accuracy.

3. Variational SEASAT Data Analysis Technique

In this section, we will discuss how the SEASAT-derived wind data can be utilized in a variational adjustment technique to help improve the sea-level pressure analysis.

On the average, the stability conditions for the marine boundary layer can be assumed to be nearly neutral (Gray, 1972). It is therefore reasonable to assume that the SEASAT-derived wind field approximates the neutral stability vector wind at 19.5 m above sea level with an error no greater than ± 2m/s in speed and ± 20° in direction. Thus, one may expect that by using a simple marine planetary boundary layer scheme such as the geostrophic drag law, one may extract the surface pressure gradient information (equivalently, but more conveniently, the surface geostrophic wind) from the satellite-derived wind. These surface geostrophic winds may be variationally combined with the sparsely distributed observations of the surface pressure using as a weak constraint the geostrophic relation in order to yield the best estimate of the surface pressure and wind fields in the least squares sense. In Section 3a, we shall discuss the procedure we use to estimate the surface geostrophic wind from the SEASAT-derived wind. Details of the variational adjustment technique will be examined in Section 3b.

a. Estimate of the Surface Geostrophic Wind

The SEASAT-derived wind can be regarded as a reasonable approximation to the wind at 19.5 m above sea level with some random errors under a neutral stability stratification. Consequently, the simplest way to estimate the surface geostrophic wind from the SEASAT-derived wind field is to make use of the geostrophic drag law together with an empirically established relationship between the surface stress and the surface wind. The geostrophic drag law for the neutrally stratified atmospheric boundary layer is given by (Tennekes, 1973):

$$\frac{ku_g}{U_*} = \ln \frac{u_*}{fz_o} - B, \quad \text{.....(3.1)}$$

$$\frac{kv_g}{u_*} = -A. \quad \text{.....(3.2)}$$

In these equations, A=5 and B=2 (Blackadar and Tennekes, 1968), which are experimentally determined similarity constants; f is the Coriolis parameter; u_* is the frictional speed; z_o is the roughness length; u_g and v_g are the components of the surface geostrophic wind respectively parallel and perpendicular to the direction of the surface stress (see Fig. 1); and k is the von Karman constant set to a value of 0.35 (Businger et al., 1971).

By denoting the magnitude of the surface geostrophic wind as G and the angle between the surface stress and the surface geostrophic wind as α (see Fig. 1), (3.1) and (3.2) may be combined to give

$$\ln \frac{G}{fz_o} = B + \ln \frac{G}{U_*} + \left(\frac{k^2G^2}{U_*^2} - A^2\right)^{1/2}, \quad \text{.....(3.3)}$$

$$\sin \alpha = \frac{u_*A}{kG} \quad . \quad \text{.....(3.4)}$$

It is reasonable to use the well-known logarithmic wind profile relation to describe the wind in the lowest, say, 20 m of a neutral atmospheric boundary layer:

$$ku_z = u_* \ell n \frac{z}{z_o} \quad \ldots\ldots\ldots\

(i) For a given field of sea-level pressure in a selected target area over the sea, compute the associated geostrophic wind components.

(ii) Compute the vector wind field at 19.5 m using (3.3) through (3.6).

(iii) Add a normally distributed random error of zero mean and 2 m/s standard deviation to the wind speed and add another normally distributed random error of zero mean and 20° standard deviation to the wind direction of the vector wind from (ii). This new wind field shall be regarded as the simulated SEASAT-derived wind field.

(iv) The simulated SEASAT-derived wind at each grid point is converted to the surface geostrophic wind using (3.3) through (3.6). After the zonal and the meridional components of the surface geostrophic wind have been obtained, they will be employed in the variational adjustment procedure discussed in the next section.

b. Variational Adjustment Technique

Calculus of variations has been widely used in the analysis of atmospheric data and in the initialization of atmospheric prediction models since Sasaki's pioneering work (1958,1969). A few of the more recent meteorological applications can be found in Barker et al. (1977) and Baxter and Goerss (1981) among others. The essence of meteorological applications of the variational method is that differences between the observed (or objectively analyzed) values and the newly adjusted values of certain meteorological variables are minimized in a least-squares sense subject to one or more dynamical constraints such as the hydrostatic relation, the balance equation, etc. A good discussion of this method can be found in Haltiner and Williams (1980).

The variational adjustment of the SEASAT data starts with the minimization of the following functional

$$J \equiv \int_{\lambda_1}^{\lambda_2} \int_{\theta_1}^{\theta_2} \{ (u - u_s)^2 + (v - v_s)^2 + A\,(P-P_s)^2$$

$$+B\left[\left(fv - \frac{RT}{P}\,\frac{1}{a\cos\theta}\,\frac{\partial P}{\partial \lambda}\right)^2 + \left(-fu - \frac{RT}{P}\,\frac{1}{a}\,\frac{\partial P}{\partial \theta}\right)^2\right]\} \, d\theta d\lambda, \quad \ldots\ldots\ldots\ldots (3.7)$$

where u_s and v_s represent the known surface geostrophic wind components derived from the simulated SEASAT wind; P_s represents the observed surface (sea-level) pressure; a the earth's radius; λ the longitude; θ the latitude; A and B are weights; and all the other variables carry their conventional meaning. Essentially (3.7) means that we require the wind and pressure fields to be as close to the "observed" values as possible subject to the weak-form constraint of the geostrophic relation.

By letting the first variation of J vanish the following three partial differential equations are obtained:

$$A(P-P_s) + \frac{1}{P}\frac{\partial}{\partial \lambda}\left[\frac{BRT}{a\cos\theta}\left(fv - \frac{RT}{a\cos\theta}\,\frac{\partial \ell n\, P}{\partial \lambda}\right)\right]$$

$$- \frac{1}{p}\frac{\partial}{\partial \theta}\left[\frac{BRT}{a}\left(fu + \frac{RT}{a}\,\frac{\partial \ell n\, P}{\partial \theta}\right)\right] = 0 \,, \quad \ldots\ldots\ldots\ldots\ldots\ldots (3.8)$$

$$u - u_s + Bf\left(fu + \frac{RT}{a}\,\frac{\partial \ell n\, P}{\partial \theta}\right) = 0 \,, \quad \ldots\ldots\ldots\ldots\ldots\ldots (3.9)$$

$$v - v_s + Bf\left(fv - \frac{RT}{a\cos\theta}\,\frac{\partial \ell n\, P}{\partial \lambda}\right) = 0 \quad \ldots\ldots\ldots\ldots\ldots\ldots (3.10)$$

The boundary conditions associated with the P-equation are $B\left(fv - \frac{RT}{a\cos\theta}\,\frac{\partial \ell n P}{\partial \lambda}\right) = 0$ on the two boundary meridians, and $B\left(fu + \frac{RT}{a}\,\frac{\partial \ell n P}{\partial \theta}\right) = 0$ on the two boundary latitudes, which can be achieved by making B zero at appropriate boundary points.

In practice, Equations (3.8), (3.9) and (3.10) are solved in discretized form. The computational mesh used is staggered as shown schematically in Fig. 2. The grid interval is taken to be 4° longitude and 4° latitude.

4. Results of Numerical Experiments

A number of numerical experiments were designed to investigate the following aspects of the variational SEASAT data analysis technique:
(i) determination of the weights, (ii) observational density and quality of pressure data, (iii) effect of quality of wind data, and (iv) influence of the surface temperature field.

In all the numerical experiments, the target area was chosen to be the region bounded by 16°N and 32°N and by 152°W and 168°E in the Pacific Ocean. Results of each variational SEASAT data analysis were compared with a predetermined FGGE IIIB surface pressure field and its associated geostrophic wind field expressed in a mesh of 4° grid resolution. Three arbitrarily chosen data sets were used in making numerical experiments for generality

a. Determination of Weights

The first problem we faced in developing the SEASAT variational adjustment technique was to determine appropriate values for weights A and B in (3.7). Even though we knew of no clear-cut way to determine their values without resorting to numerical experiments, examination of (3.8), (3.9) and (3.10) served to shed light on how to choose them.

We first noted that, of the two weights A and B, only the latter appears in the velocity equations (3.9) and (3.10). That implies that B is to mainly control to what degree wind data are allowed to deviate from (u_s, v_s). A vanishing value of B means that no adjustment of wind data is to take place. Larger values of B,

on the other hand, allow for increasing adjustment of wind data according to the geostrophic constraint. By collecting terms in (3.9) and (3.10), we found that coefficients for u and v are both $1+Bf^2$, where f is the Coriolis parameter. Thus, by making Bf^2 orders of magnitude smaller or larger than unity, we may either force the wind data to stay to be (u_s,v_s) or make the wind to be adjusted geostrophically. By assigning a typical value of 1.E-4 S^{-1} to f and by allowing Bf^2 to vary between 1.E2 and 1.E-2, we found the proper range of B values to be between 1.E6 and 1.E10 S^2. Therefore, we chose to employ five discrete levels of B values: 1.E6, 1.E7, 1.E8, 1.E9 and 1.E10 S^2 in the numerical experiments for determining the most appropriate value for B.

Having obtained the range of B values, we next need to determine the range of the A values to be used with a given B. The key point to consider was that the observational density of the surface pressure data is rather low over ocean areas. In the current framework, that means that values of P_s are only available at a few grid points in a large domain and surface pressure values at all other grid points need to be obtained from the SEASAT-derived wind data. In order for these to hold, a very small value of A (effectively zero) needs to be assigned to those grid points without pressure observations. On the other hand, a large-enough value of A must be designated to grid points with pressure data. Since A is effectively zero at grid points where P_s were not given, when we refer to the value of A, we shall mean the A value for grids with pressure observations from this point on.

The following pieces of information are associated with the numerical experiments for determining Weights A and B: The computational domain was chosen to be the area bounded by 16°N, 32°N, 152°W and 168°E in the Pacific Ocean. The grid resolution in this area was chosen to be 4° so that the domain was composed of a

total of 5 x 11 grid points. Seven of the fifty-five grid points were assumed to have pressure observations. See Fig. 3 for locations of the pressure observations. This figure also shows that the entire domain is rather uniformly spanned by the seven observations. The observed wind and pressure data were assumed to contain errors, and these errors were assumed to be normally distributed with standard deviations in wind speed, wind direction and pressure to be respectively 2 m/s, 20° and 1 mb. Plots of the surface pressure fields of February 25, March 1 and March 9, 00z, 1979 are respectively shown in Figs. 4, 5 and 6. Also included in these figures are the zonal and meridional differences between the true geostrophic and the unadjusted wind data.

Pressure and wind fields were computed for five levels of B against six levels of B/A for each data set. The reason we used the ratio B/A is because (3.8) can be scaled by either A or B, therefore only the ratio B/A is of importance in solving this equation. Pressure and wind RMS errors were computed and listed in Tables 1, 2, and 3 for the three data sets, respectively. The wind RMS error is defined to be the sum of the u- and the v-RMS errors. Inspection of the pressure RMS error in these three tables reveals that accuracy of the final pressure field is rather insensitive to the choice of B. The dependence of the pressure RMS error on B/A also seems to be rather weak so long as B/A is smaller than 1.E20 S^2g/m^3. When the values of B/A exceeds this threshold value, significant increase in pressure RMS error may occur, which implies that the difference between P and P_s at grid points with pressure data has been allowed to become undesirably large. Before we examine the wind RMS error in these tables, it is necessary to know that the wind RMS error for the unadjusted wind field (u_s, v_s) was found to be, respectively, 3.9, 4.8 and 5.5 m/s for the three data sets. By comparing these values with the wind RMS error in Tables 1, 2 and 3, we find that

in the high-B case (1.E10 S^2), a significant reduction in RMS error was resulted as compared with the intermediate-B (1.E8 S^2) and the low-B (1.E6 S^2) cases. This general trend is observable in all three data sets. The dependence of the wind RMS error on B/A is seen to be in phase with the pressure RMS error. From the above results, it seems reasonable to choose B to be 1.E10 S^2 and B/A to be 1.E19 S g/m^3 as the appropriate values. Or equivalently, B = 1.E10 S^2 and A = 1.E-9 m^3/g are the chosen values for the weights. As a result, these two values were used in making all the numerical experiments from this point on. The fact that the pressure RMS error is insensitive to the choice of B whereas a smaller wind RMS error is resulted in the high B case as compared with the low-B case suggests two things: (i) Errors embedded in the wind data make the wind field less geostrophic. Therefore, by imposing the geostrophic constraint, an improved wind field can be obtained. (ii) If a low value of B is used, the pressure field resulted will differ very little from the pressure field obtained for a high-B value. The geostrophic wind field computed for the resultant pressure field in the low-B case will give almost the same adjusted wind field as in the high-B case.

Choice of the most appropriate A value in the above discussion was made on the basis of a 1 mb random error embedded in the pressure data. In order to determine whether or not this value of A is also applicable to cases with smaller random errors in the pressure data, pressure and wind RMS errors were also computed in the case of perfect pressure data for B=1.E10 S^2 against five levels of A values. The result is presented in Table 4. Inspection of this table indicates that when pressure data contain no error in them, the wind and pressure RMS errors both decrease, but their general dependence on A still holds. Therefore, the choice A = 1.E-9 m^3/g, B = 1.E10 S^2 can actually be used for

pressure observations with a standard deviation of errors ranging from zero to 1 mb.

For ease of making graphical comparisons, plots of the difference fields between the adjusted and the true pressure, zonal wind and the meridional wind using the three data sets are respectively presented in Figs. 7, 8 and 9. It is noteworthy that areas of large pressure RMS errors seem to be well related to areas of strong pressure gradient, as can be seen by comparing Figs. 4, 5, 6 and Figs. 7, 8, 9. This point will be mentioned again in the next subsection.

b. Observational Density and Quality of Pressure Data

We may expect that results of the SEASAT analysis technique would become more accurate with more pressure observations. This expectation is strictly valid if no error is contained in the pressure data. However, because errors indeed appear in the pressure data as a result of human and instrumental errors in addition to pressure perturbations due to the presence of subsynoptic-scale atmospheric features, the validity of the above expectation may only hold in a statistical sense. This consideration inspired us to study effects of the observational density and quality of pressure data on the accuracy of the SEASAT analysis technique. Another reason for studying this subject is that it is desirable to get a rough estimate of the minimal number of pressure observations in a typical ocean area, say, expanded by 5 x 11 4°-resolution mesh points, which is required to provide a reasonable pressure analysis in the current SEASAT analysis technique.

As was mentioned before, quality of the pressure data is controlled in the current framework through assigning different numerical values to the standard deviation of the normally distributed random errors of zero mean. In the following numerical experiments, the standard deviation of pressure errors was chosen to

be 1 mb. However, before the random errors generated by a call to a random number generator were added to the true pressure values, they were multiplied by values of 1, 0.5, 0, -0.5, and -1 to simulate varying degrees of accuracy of the pressure data. Cases associated with these five numbers will be referred to as the "+1", "+0.5", "0", "-0.5" and "-1" cases. Each case was run for a total of 3, 5, 7, 9 and 11 pressure observations. In each run, pressure observations were located such that the domain was approximately unifomly covered by the pressure data points. Moreover, in the three- and the five-point cases, for instance, the former formed a subset of the latter. This holds true for up to the eleven-point case. Positions of the eleven pressure observations are schematically shown in Fig. 3. Locations of the pressure data are numbered in this figure to help illustrate which points to use for the three-, five-, up to the eleven-point cases.

The resultant pressure and wind RMS errors for the above experiments are summarized in Tables 5, 6 and 7 respectively for the three data sets used. It can be seen that all three tables show very similar behaviors of the pressure and wind RMS errors. Therefore, we only need to use Table 5 to discuss the error pattern. We first examine the pressure RMS error. It is clear that when no error is contained in the pressure data, the pressure RMS error shows a gradual decrease with increasing pressure observations as shown in the "0" case. This slow pace of reduction in the pressure RMS error implies that if pressure data are error-free, then as low as three pressure observations in conjunction with SEASAT-derived wind data in a 5 x 11 grid domain may suffice to generate a reasonably accurate pressure analysis. A moderate increase in observational density of pressure data may only lead to a slightly improved pressure analysis. When pressure data contain random errors of standard deviation of 0.5 mb, we used the "+ 0.5" and the

"-0.5" cases to illustrate the behavior of the pressure RMS error. It can be seen in Table 5 that values of the pressure RMS error in the "+ 0.5" and "-0.5" cases are considerably different when only three pressure data are available. This difference is considered to signify insufficient pressure data in the SEASAT data analysis technique. As expected, this difference becomes less prominent with increasing pressure observations. Another measure of the sufficiency of pressure data can be obtained as follows: Compute the average pressure RMS error in the "+0.5" and "-0.5" cases, and compare it with the pressure RMS error in the "0" case. The former is usually larger than the latter, and their difference measures the scatteredness of the pressure RMS error and the sufficiency of the pressure data. It is seen that, in a statistical sense, the pressure RMS error becomes smaller and less scattered when the number of pressure data was increased from three to five. Further increases of this number to seven, nine and eleven do not show significant improvement in accuracy of the final pressure field. In the "+1" and "-1" cases, the behavior of the pressure RMS error is very similar to that in the "+0.5" and "-0.5" cases except for a larger magnitude and a more scattered pattern of this error. On the basis of the above discussions, we conclude that in the current SEASAT data analysis technique, no more than seven uniformly located pressure data are required in the domain to produce a reasonably accurate pressure analysis. Moreover, an upgrade in quality of the pressure data can definitely give rise to an improved pressure analysis and is, therefore, highly desirable. This point will be reiterated in passing.

Having examined the pressure RMS error in Tables 5, 6, and 7, we may now inspect the wind RMS eror. In the "0" case, the wind RMS error shows an extremely slow decrease with increasing observations. Actually, the rate of decrease is so slow that we may simply consider the wind RMS error in the "0" case to be indepen-

dent of the number or pressure observations available. The implication here is that the observational density of pressure data in these cases is too low to provide enough pressure gradient information to help improve the wind data. This is so when the pressure data are error-free. If pressure data contain errors, then erroneous pressure gradient information may actually be passed into the wind data, so that the adjusted wind field may show a larger wind RMS error when more and more pressure observations are used in the current technique. This can be seen to have happened in cases of eleven pressure observations in Tables 5, 6, and 7. As a result, if the wind data are to be adjusted according to the geostrophic constraint, it is advisable to use only two or three pressure data in the current scheme to avoid an adverse feedback from errors in the pressure data.

In the above discussions, locations of pressure data were chosen to cover the domain approximately in a uniform manner. It was also shown that in such circumstances, a moderate increase in the number of pressure observations did not result in significantly improved accuracy of the final pressure analysis very efficiently. As was pointed out in the previous subsection that areas of large pressure RMS errors and areas of strong pressure gradient seem to be well correlated. This observation inspired us to speculate that perhaps an improved pressure analysis can be obtained by making some additional pressure observations in places of special significance such as areas of strong pressure gradient (designated by observed strong surface wind). Bearing this in mind, we conducted a few numerical experiments to be discussed below to clarify things: The case associated with Fig. 7 that used the February 25 data with seven pressure observations is used as the control case. Three runs with an additional pressure observation added to the original seven pressure data were made for making comparisons. The position of this additional pressure observation was located at

the point marked by an "x" in Fig. 3, where very strong pressure gradient exists as can be seen in Fig. 4. Values of the standard deviation of the random pressure errors in the three runs were,respectively, 1, 0.5 and 0 mb. The wind errors were kept at 20° and 2 m/s in direction and speed. Pressure RMS errors in these three runs were found to be 0.67, 0.48 and 0.36 mb. When these numbers are compared with the corresponding pressure RMS errors in the seven-point case in Table 5, it is seen that for pressure random errors of standard deviation of 1 mb, there is hardly any improvement in the final pressure analysis by including the eighth pressure observation. However, for pressure random errors of standard deviation of 0.5 mb, significant improvement in the pressure analysis is seen to result from the inclusion of this additional pressure data point. For error-free pressure data, the improvement is further enhanced. Thus, it can be concluded that a judicious placement of positions of the pressure observations may result in markedly improved pressure analysis in the current work, provided that the quality of the pressure data is characterized by random errors no greater than 0.5 mb. Plots of the difference between the adjusted and the true pressure fields in the above three cases are shown in Fig. 10 for comparison purposes.

c. Effect of Quality of Satellite-Derived Wind Data

If a new satellite like SEASAT is launched into space in the future, refined sensing devices can be expected to be on board to help resolve the true surface wind over ocean areas. Consequently, wind data derived from the satellite observations are expected to be more accurate than today's wind data. The impact of improved satellite-derived wind data on the accuracy of the current pressure analysis technique can be assessed by reducing the magnitude of errors embedded in wind speed and direction. For this purpose, a few additional numerical experiments were run using the February 25 data with seven pressure observations. Listed

in Table 8 are five cases with different values of the error standard deviations in pressure and wind data. By comparing Cases 1 and 3, we see that the pressure RMS error is reduced from 0.65 mb to 0.52 mb or a 20% reduction, when there is a 50% reduction of the wind error in both speed and direction. Further reductions in wind random errors will no longer significantly reduce the pressure RMS error as is indicated by comparing Case 3 with Case 5. Cases 1 and 2 show that a 20% reduction in pressure RMS error is also obtainable when there is a 50% reduction in pressure random errors. However, the most effective way in reducing the pressure RMS error is to simultaneously reduce the random errors in wind and pressure data by 50%. That way, a 50% reduction in pressure RMS error is resulted as evidenced by comparing Cases 1 and 4. On the basis of these discussions, we come to the conclusion that it is desirable to upgrade the quality of the satellite-derived wind data. However, there is an upper limit on the accuracy of the resultant pressure analysis by merely reducing random errors in the wind data. If a reduction of errors in the pressure data takes place along with an upgrade of the wind data, the resultant pressure analysis will have a much higher accuracy

ontour plots of the difference fields between the observed and the true pressure and the zonal and the meridional wind components are presented in Fig. 11 for completeness.

d. Influence of the Surface Temperature Fields

In all the previous numerical experiments discussed, we have tacitly assumed that the surface temperature field is completely known at every grid point in the domain. However, unless the sea surface temperature field is already obtained elsewhere, say, by blending the satellite temperature observations into the conventional data, temperature can only be known at those grid points where surface pressure is observed. When this is not the case, a convenient alternative is to

use a constant temperature field in the current analysis scheme. This constant temperature can be chosen as, for instance, a representative mean temperature of the entire domain. We made three additional runs in order to find out how much influence this may have on the outcome of the SEASAT pressure analysis. The control case is again the one using the true surface temperature field and seven pressure observations as was shown in Fig. 6. The random erors in wind speed, wind direction and pressure data were assumed to have standard deviation 2 m/s, 20° and 1 mb. The data set chosen was of February 25, 00z, 1979. In the three runs we made, the constant temperature was respectively chosen as 300, 283, and 291°K, the last being the average of the seven surface temperature observations given. The 300 and 283°K temperatures were employed to represent more extreme cases. The resultant pressure RMS errors were found to be 0.67, 0.68 and 0.69 mb, respectively for the 283, 291 and 300°K temperatures. These values are to be compared with the pressure RMS error in the control case, which is 0.65 mb. It is clear that use of a constant temperature field in the SEASAT data analysis scheme, in the worst case, only gives rise to a 6% error in the pressure analysis. We, consequently, conclude that it is viable to use a representative constant temperature field when temperature observations are not readily available in the entire domain. For ease of making graphical comparisons of the resultant pressure RMS error in each case, plots of the difference fields from the true pressure solution for the three constant temperatures are shown in Fig. 11. The three error fields are seen to be very similar to one another to corroborate our conclusion.

5. Concluding Remarks

The SEASAT-derived wind can be considered as the neutral stability vector

wind at 19.5 m above sea level with an accuracy of ±2 m/s and ±20° respectively in speed and direction. These errors are considered characteristic and were used in simulating the SEASAT-derived surface wind data from the geostrophic wind field associated with a chosen surface pressure field in an ocean area. With the aid of the simple geostrophic drag line and an empirical formula for the netural stability drag coefficient, the simulated SEASAT-derived wind data were converted to the corresponding surface geostrophic wind at 10 m above the sea level. The marine boundary layer scheme used in the current study is not intended to be very accurate but only a simple scheme. A variational problem with the geostrophic wind relation as the weak constraint was then formed to combine the sparse surface pressure data with the dense satellite-derived wind data. After this variational problem was solved numerically, the resultant pressure field was compared with the true pressure field and the adjusted wind field was compared with the geostrophic wind field associated with the true pressure field. In conducting the current study, the following have been observed or concluded.

(1) Weight B, in the current work, controls the degree of the geostrophic constraint is imposed. If B is chosen to be 1.E10 S^2 or larger, the adjusted wind field will become highly geostrophic, but if B is chosen to be 1.E6 S^2 or smaller, little geostrophic adjustment of the wind will occur and the wind will remain very close to (u_s, v_s).

(2) For any given B value, there is a corresponding threshold value of A existing. For an A value exceeding this threshold, the resultant pressure field may become rather inaccurate because the difference between the resultant pressure and the observed pressure is allowed to be unsoundly large in this case, which is undesirable.

(3) A and B were respectively chosen to be 1.E-9 m^3/g and 1.E10 S^2 as the most

appropriate values in the current work. However, the fact that the pressure RMS error is seen to be quite insenstitive to B whereas the wind RMS error in the high-B case is considerably smaller than in the low-B case suggests that very similar wind and pressure fields can be obtained in a low-B case if the geostrophic wind computed from the resultant pressure field is used to replace the unadjusted wind data (u_s, v_s). The implication of this is that random erors in the wind data can be partially removed by enforcing the geostrophic constaint.

(4) When wind data are geostrophically adjusted to reduce embedded errors, it is best to use only two or three pressure observations in the current technique. The reason is that when errors appear in the pressure data, they may result in false pressure gradient information to make the adjusted wind even less accurate than the unadjusted wind. This will become more serious when more pressure data are available as larger pressure gradient errors can be expected.

(5) For a domain of 5 x 11 grid points, no more than seven unifomly located pressure observations are needed when used in conjunction with the SEASAT-derived wind data to result in a reasonably accurate pressure analysis. A moderate increase in pressure observations, say from seven to eleven, cannot do much in improving accuracy of the pressure analysis especially when pressure data contain sizeable random errors. This suggests that efforts to reduce errors embedded in the pressure data are worthwhile for obtaining improved pressure analysis in the current technique.

(6) If it is possible to obtain a limited number of surface pressure observations anywhere in the oceans, then it is advisable to make a few observations in areas of strong pressure gradient as designated by strong satellite-derived

surface wind. It was shown that judicious placement of pressure observational points in these areas may result in significant improvement in the pressure analysis.

(7) An upgrade of the satellite-derived wind data may give rise to an improved pressure analysis. However, it will be more effective to improve the pressure analysis if the quality of both the wind and the pressure data can be simultaneously upgraded.

(8) Use of a representative constant temperature fields in the current data analysis technique results in no more than 6% error in the final pressure analysis. Therefore, it is viable to use a mean temperature in the entire domain if temperature observations are not available at very grid point.

Table 1. Pressure and wind RMS errors in mb and m/s computed for the February 25, 00Z, 1979 data. Two numbers are given for each pair of B and B/A values, the upper one being the pressure RMS error and the lower one being the wind RMS error. The wind RMS error for (u_s, v_s) was found to be 3.90 m/s. Standard deviations of the random errors embedded in wind speed, wind direction and pressure are respectively 2 m/a, 20° and 1 mb.

$B/A(S^2g/m^3)$ \ $B(S^2)$	1.E10	1.E9	1.E8	1.E7	1.E6
1.E14	0.69	0.66	0.65	0.64	0.64
	3.27	3.25	3.52	3.83	3.89
1.E17	0.69	0.66	0.63	0.61	0.61
	3.27	3.25	3.52	3.84	3.89
1.E18	0.67	0.64	0.59	0.57	0.57
	3.29	3.23	3.52	3.84	3.89
1.E19	0.65	0.60	0.58	0.57	0.57
	3.25	3.18	3.54	3.85	3.89
1.E20	0.60	0.66	0.71	0.70	0.63
	3.15	3.19	3.56	3.85	3.89
1.E21	1.10	1.36	1.08	1.07	1.07
	3.14	3.21	3.56	3.85	3.89

Table 2. Same as Table 1 except for March 1, 00Z, 1979 data. The velocity RMS error of (u_s, v_s) is 4.79 m/s.

B/A(S^2g/m^3) \ B(S^2)	1.E10	1.E9	1.E8	1.E7	1.E6
1.E14	0.91	0.91	0.92	0.94	0.94
	4.05	3.98	4.24	4.69	4.78
1.E17	0.91	0.91	0.92	0.94	0.94
	4.04	4.03	4.27	4.70	4.78
1.E18	0.91	0.81	0.92	0.94	0.93
	4.03	4.00	4.27	4.70	4.78
1.E19	0.90	0.92	0.98	1.01	1.00
	4.05	3.92	4.27	4.71	4.78
1.E20	0.93	0.98	1.03	1.05	1.05
	3.92	3.91	4.28	4.71	4.78
1.E21	1.91	1.85	1.86	1.87	1.87
	3.94	3.92	4.30	4.71	4.78

Table 3. Same as Table 1 except for March 9, 00Z, 1979 data. The velocity RMS error of (U_s, v_s) is 5.50 m/s

$B/A(S^2g/m^3)$ \ $B(S^2)$	1.E10	1.E9	1.E8	1.E7	1.E6
1.E14	0.80	0.80	0.84	0.85	0.85
	4.32	4.27	4.70	5.36	5.49
1.E17	0.80	0.80	0.84	0.86	0.84
	4.32	4.27	4.66	5.35	5.69
1.E18	0.80	0.81	0.82	0.84	0.86
	4.32	4.24	4.67	5.35	5.49
1.E19	0.81	0.79	0.83	0.86	0.86
	4.28	4.18	4.72	5.36	5.49
1.E20	0.79	0.83	0.86	0.88	0.86
	4.29	4.22	4.74	5.37	5.49
1.E21	0.89	0.91	0.89	0.91	0.91
	4.33	4.25	4.74	5.49	5.69

Table 4. Pressure and wind RMS errors in mb and m/s for B = 1.E10 S^2 and five levels of A. The standard deviations of random errors embedded in wind speed, wind direction and pressure are, respectively, 2 m/s, 20° and 0 mb.

A (m^3/g)	Data Set FB25	MR01	MR09
0.1E-5	0.63	0.64	0.47
	3.85	4.14	3.07
0.1E7	0.63	0.64	0.47
	3.85	4.14	3.07
0.1E-8	0.63	0.63	0.47
	3.85	4.15	3.07
0.1E-9	0.66	0.63	0.49
	3.87	4.16	3.09
0.1E-10	1.46	0.68	0.73
	3.94	4.23	3.13

Table 5. Presure and wind RMS errors in mb and m/s for different numers of pressure observations against different data qualities computed for the February 25 data.

Pressure Stnd Dev. (m/b)	No. of Pressure Observations				
	3	5	7	9	11
1	0.67	0.68	0.65	0.71	0.60
	3.26	3.24	3.25	3.35	3.74
0.5	0.45	0.53	0.53	0.52	0.48
	3.15	3.13	3.11	3.11	3.21
0	0.54	0.50	0.47	0.46	0.46
	3.11	3.11	3.07	3.03	3.03
-0.5	0.80	0.61	0.53	0.58	0.56
	3.13	3.16	3.12	3.11	3.23
-1	1.13	0.81	0.67	0.80	0.73
	3.24	3.29	3.27	3.36	3.76

Table 6. Same as Table 5 except for March 1 data

Pressure Stnd Dev. (m/b)	No. of Pressure Observations				
	3	5	7	9	11
1	1.03	1.03	0.90	0.94	0.81
	4.05	4.01	4.02	4.04	4.38
0.5	0.84	0.82	0.74	0.72	0.66
	3.95	3.91	3.89	3.85	3.92
0	0.72	0.68	0.63	0.57	0.56
	3.92	3.88	3.85	3.78	3.78
-0.5	0.66	0.63	0.61	0.58	0.57
	3.95	3.91	3.89	3.95	3.96
-1	0.70	0.70	0.67	0.73	0.67
	4.05	4.02	4.02	4.04	4.42

Table 7. Same as Table 5 except for March 9 data

Pressure Stnd Dev. (m/b)	No. of Pressure Observations				
	3	5	7	9	11
1	0.83	0.77	0.79	0.84	0.75
	4.35	4.33	4.30	4.44	4.65
0.5	0.69	0.65	0.68	0.67	0.64
	4.26	4.22	4.29	4.16	4.23
0	0.64	0.64	0.63	0.61	0.61
	4.23	4.19	4.19	4.19	4.09
-0.5	0.66	0.74	0.68	0.70	0.68
	4.26	4.22	4.17	4.14	4.24
-1	0.79	0.91	0.79	0.90	0.82
	4.35	4.31	4.27	4.30	4.66

Table 8. Pressure RMS error for various qualities of pressure and wind data.

Case No.	Error Standard Deviation			Pressure RMS error (mb)
	Wind Direction (°)	Wind Speed (m/s)	Pressure (mb)	
1	20	2	1	0.65
2	20	2	0.5	0.53
3	10	1	1	0.52
4	10	1	0.5	0.32
5	0	0	1	0.48

FIGURE CAPTIONS

Fig. 1 Schematic representation of the geostrophic drag law. α is the angle between the surface stress and the geostrophic wind.

Fig. 2 Schematic of the staggered mesh used in conducting the SEASAT variational data analysis.

Fig. 3 Schematic illustration of the computational domain and locations of surface pressure observations. The "x" gives the location of the additional pressure observation used in obtaining results plotted in Fig. 10.

Fig. 4 Contour plots of the true surface pressure in 1 mb intervals (top), plot of the difference between u_s and u_{true} in 1 m/s intervals (middle), and plot of the difference between v_s and v_{true} in 2 m/s intervals (bottom). The data set used is of February 25, 00Z, 1979.

Fig. 5. Same as Fig. 4 except for the March 1, 00Z, 1979 data set.

Fig. 6 Same as Fig. 4 except for the March 9, 00Z, 1979 data set.

Fig. 7 Contour plot of the difference between P and P_{true} in 0.2 mb intervals (top), plot of the difference between u and u_{true} in 2 m/s intervals (middle), and plot of the difference between v and v_{true} in 2 m/s intervals (bottom) for the February 25, 00Z, 1979 data.

Fig. 8 Same as Fig. 7 except for the March 1, 00Z, 1979 data.

Fig. 9 Same as Fig. 8 except for the March 9, 00Z, 1979 data.

Fig. 10 Contour plot of the difference between P and P_{true} in 0.2 mb interals for the February 25, 00Z, 1978 data. Eight pressure observations are used in the data analysis. See Fig. 3 for the location of the additional pressure observation. The standard deviations of rndom erros are 20° in wind direction and 2 m/s in wind speed. The standard deviations of pressure random errors are 1 mb (top), 0.5 mb (middle) and 0 mb (bottom).

Fig. 11 Contour plot of the difference between P and P_{true} in 0.2 mb intervals for the February 25, 00Z, 1978 data. Seven pressure observations are used. The standard deviations of the wind and pressure random errors are 20°, 2 m/s and 0.5 mb (top), 10°, 1 m/s and 1 mb (middle), and 10°, 1 m/s and 0.5 mb (bottom).

Fig. 12 Contour plot of the pressure difference between P and P_{true} in 0.2 mb intervals for the February 25, 00Z, 1979 data. Seven pressure observations are used, and the wind and pressure random errors are 20°, 2 m/s and 1 mb. A constant temperature field of 200°K is used in obtaining the top plot, 291°K in the middle plot and 283°K in the bottom plot.

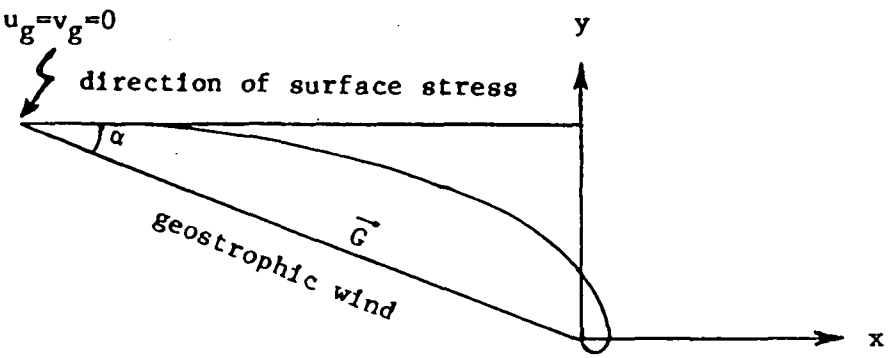

$u_g=v_g=0$
y
direction of surface stress
α
$\widetilde{G}$
geostrophic wind
x

Fig. 1

ORIGINAL PAGE IS
OF POOR QUALITY

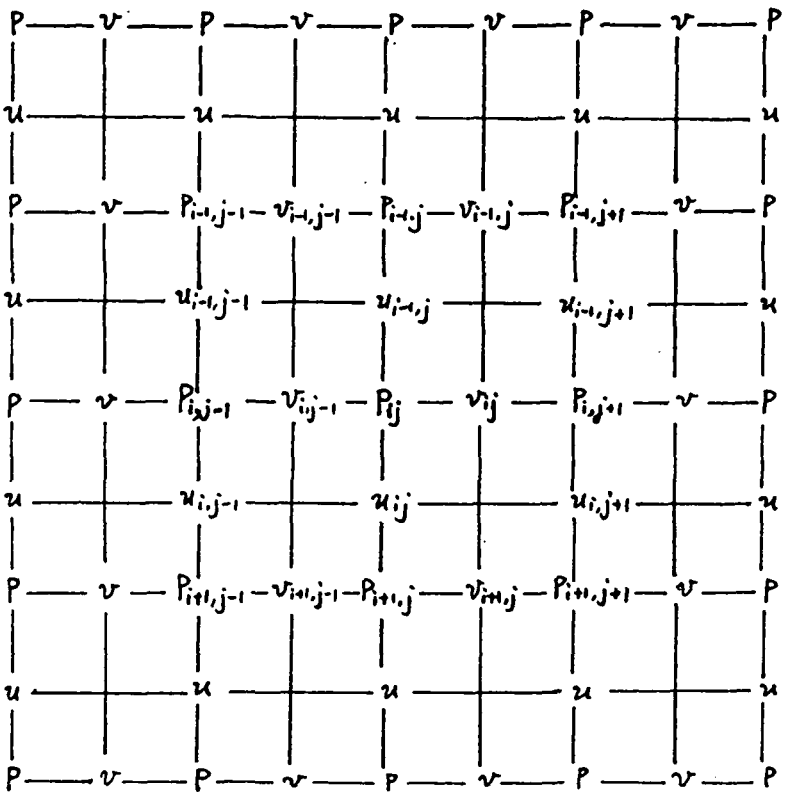


Fig. 2

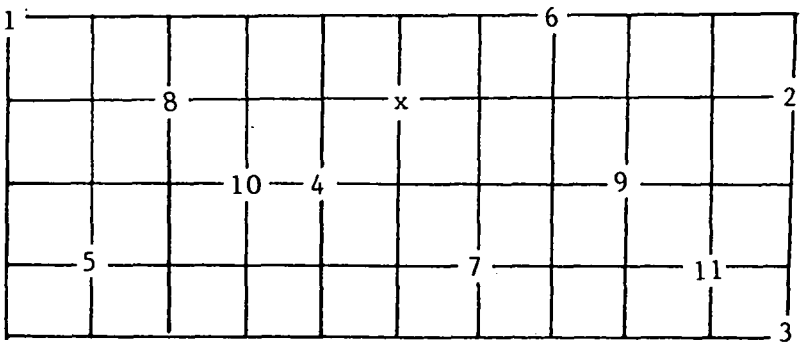
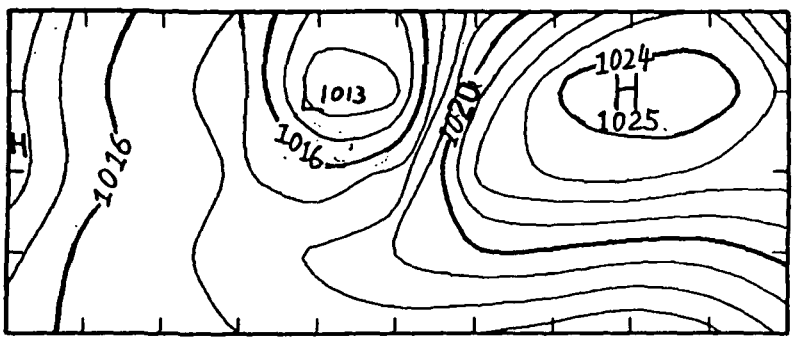
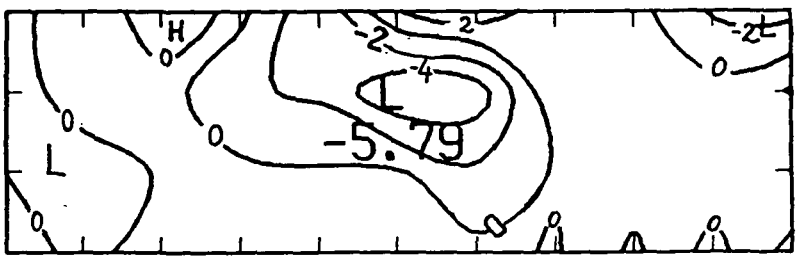


Fig. 3


1013
1016
1016
1020
1024
H
1025.


H
0
-2
2
-4
L
-5.79
0
0
L
0
-2
0
0
0

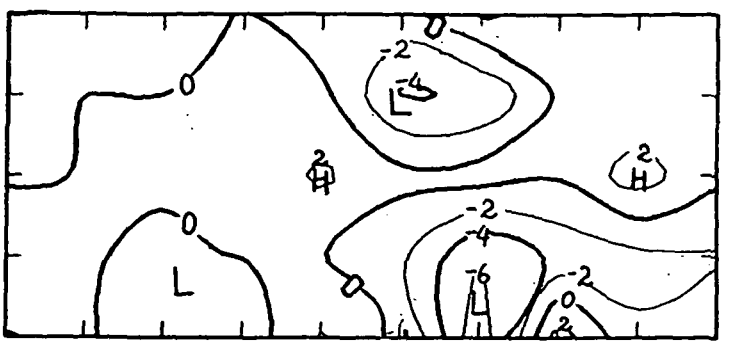
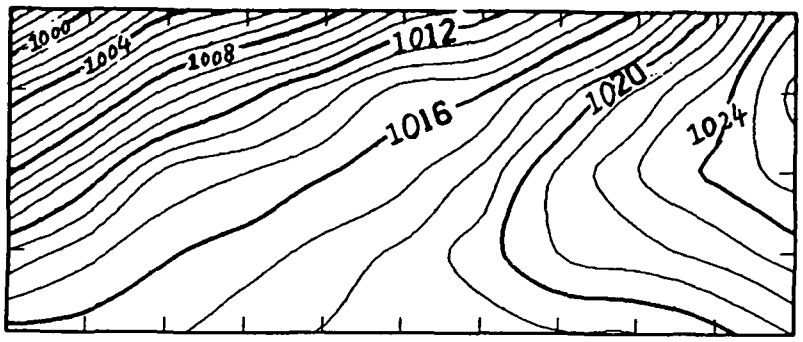
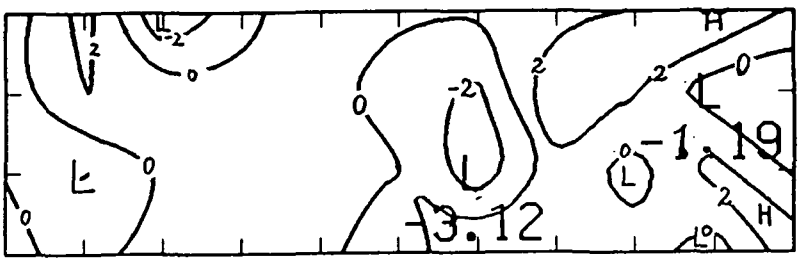

0
-2
L
0
2
H
2
H
-2
-4
0
L
-6
H
-2
0
2

Fig. 4





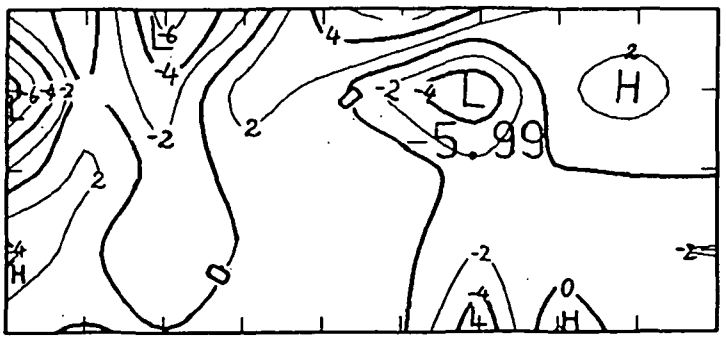
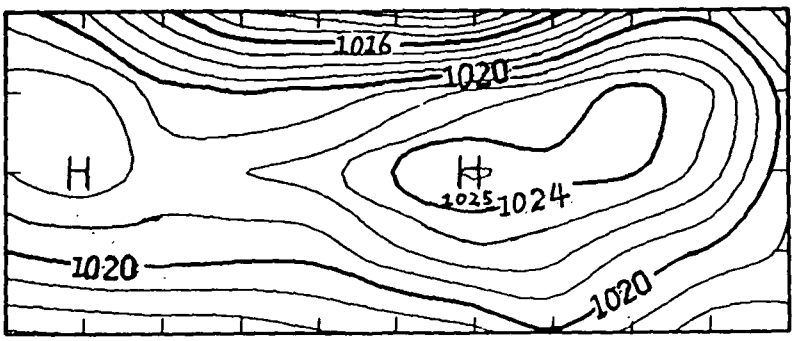
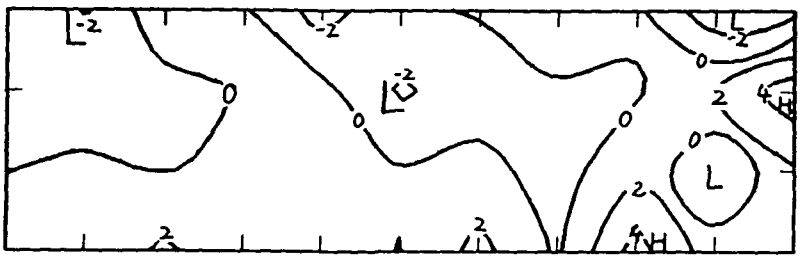


Fig. 5





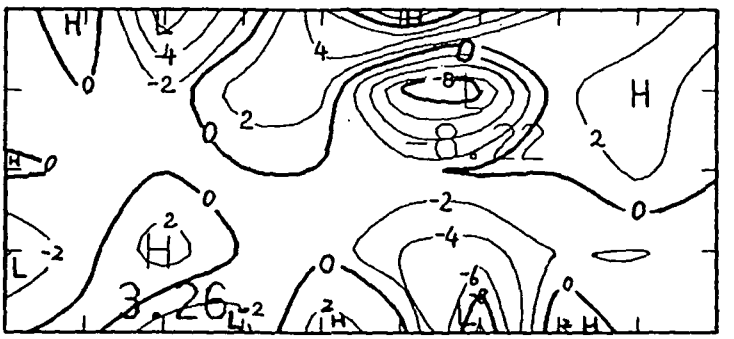
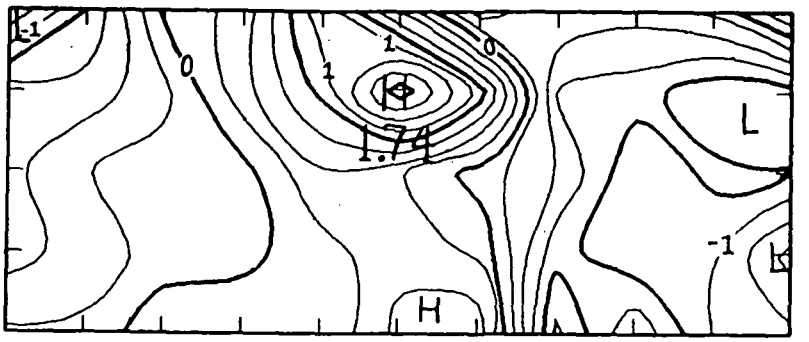
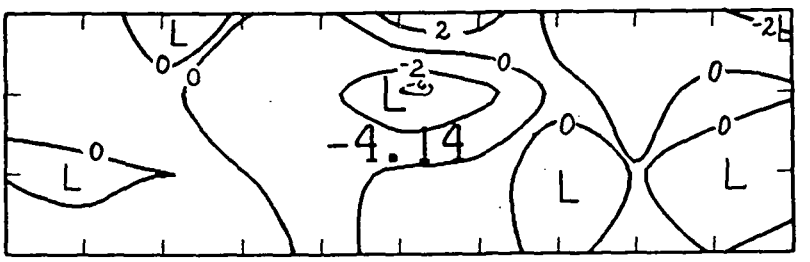


Fig. 6





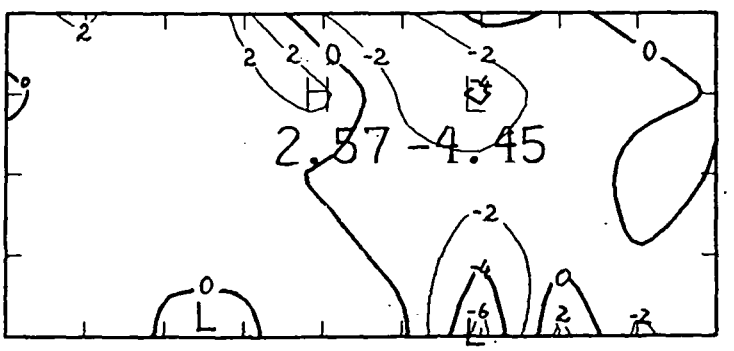


Fig. 7

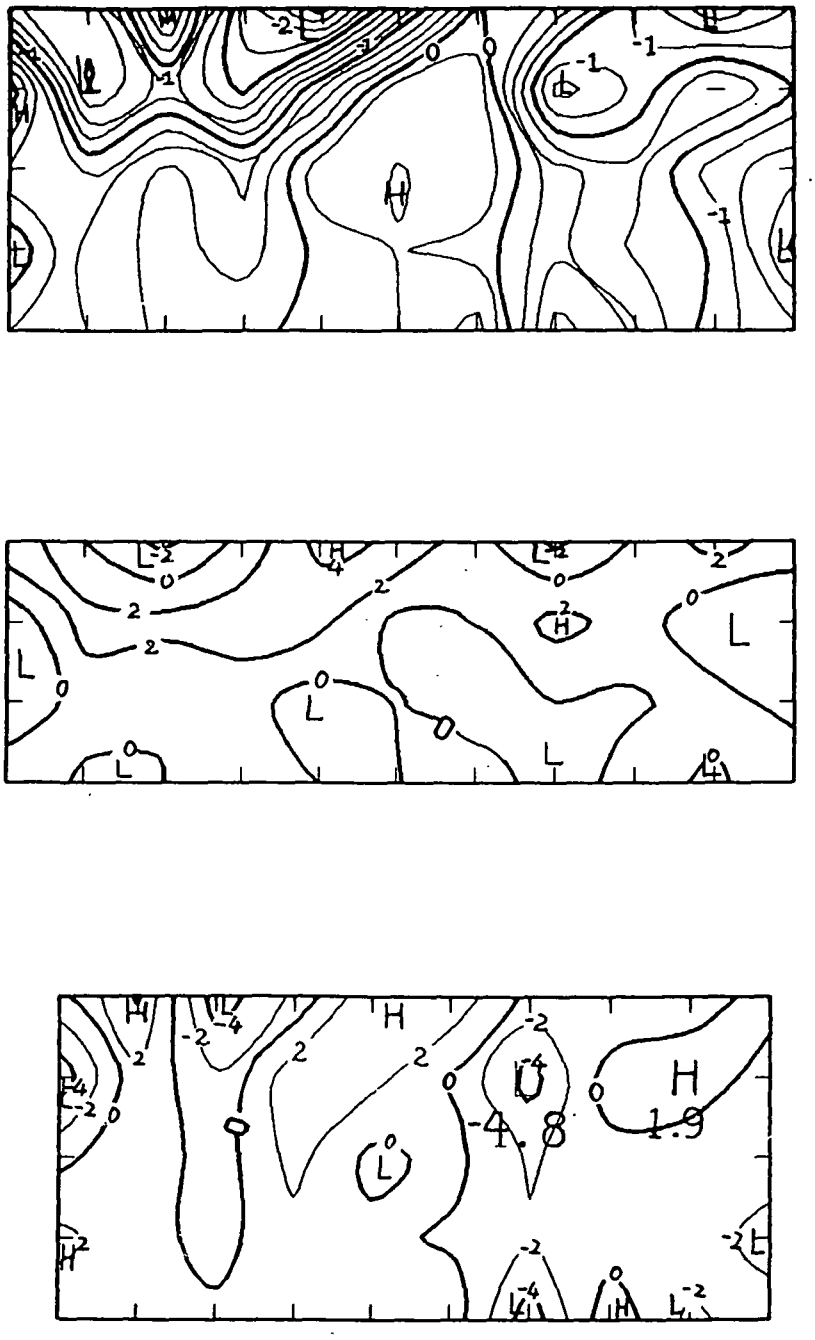


Fig. 8

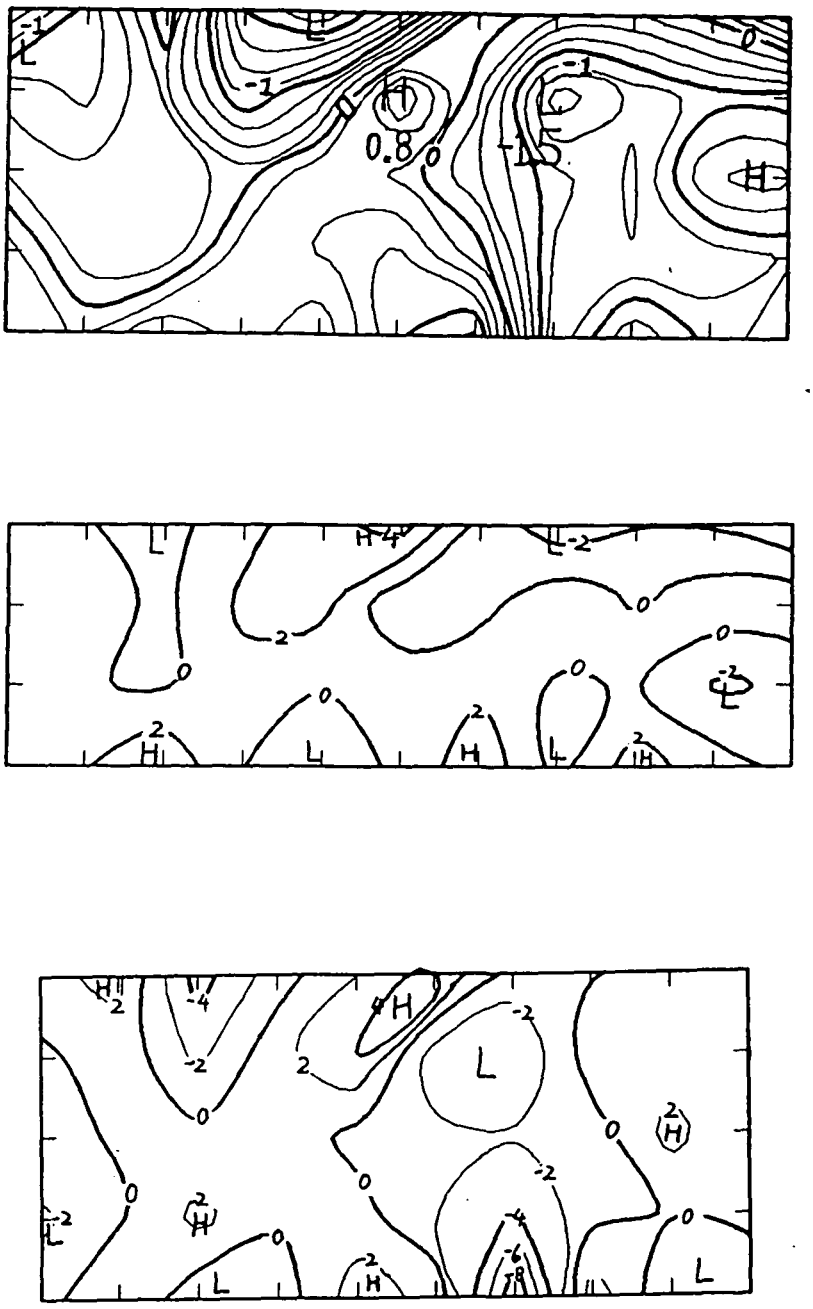

-1
L
-1
0
H
0.8
0
-1
L
-1.0
H
H
4
L
-2
0
-2
0
0
0
-2
L
2
H
0
L
2
H
0
L
2
H
H
2
-4
H
0
-2
-2
2
L
0
2
H
0
0
-2
-2
L
2
H
0
-4
-6
L
L

Fig. 9

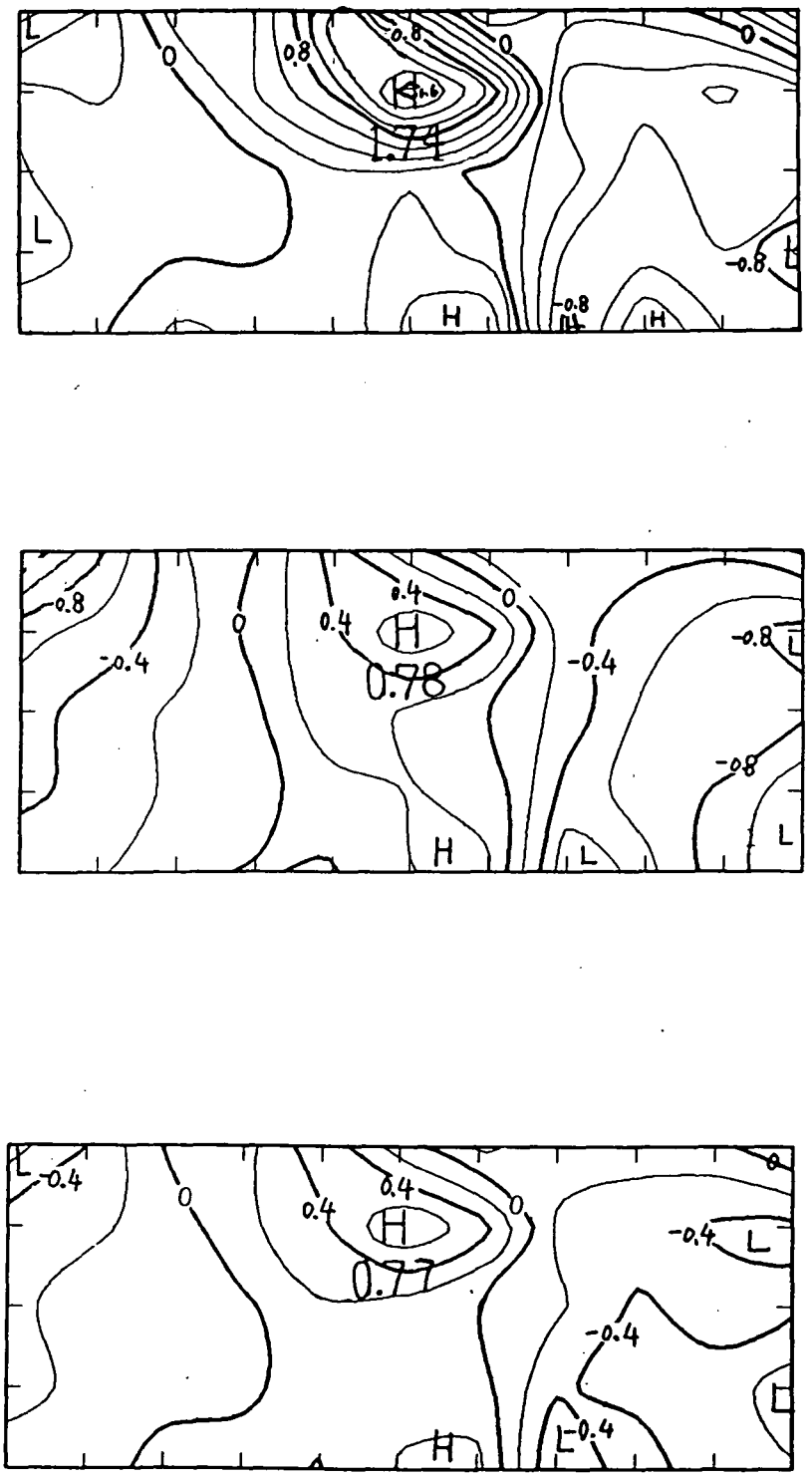

L
0
0.8
0.8
0
0
H
1.74
L
-0.8
L
H
-0.8
H
0.8
0
0.4
0
H
0.78
-0.4
-0.4
-0.8
L
H
L
L
-0.8
-0.4
0
0.4
0.4
0
H
0.77
-0.4
L
-0.4
H
L
-0.4

Fig. 10

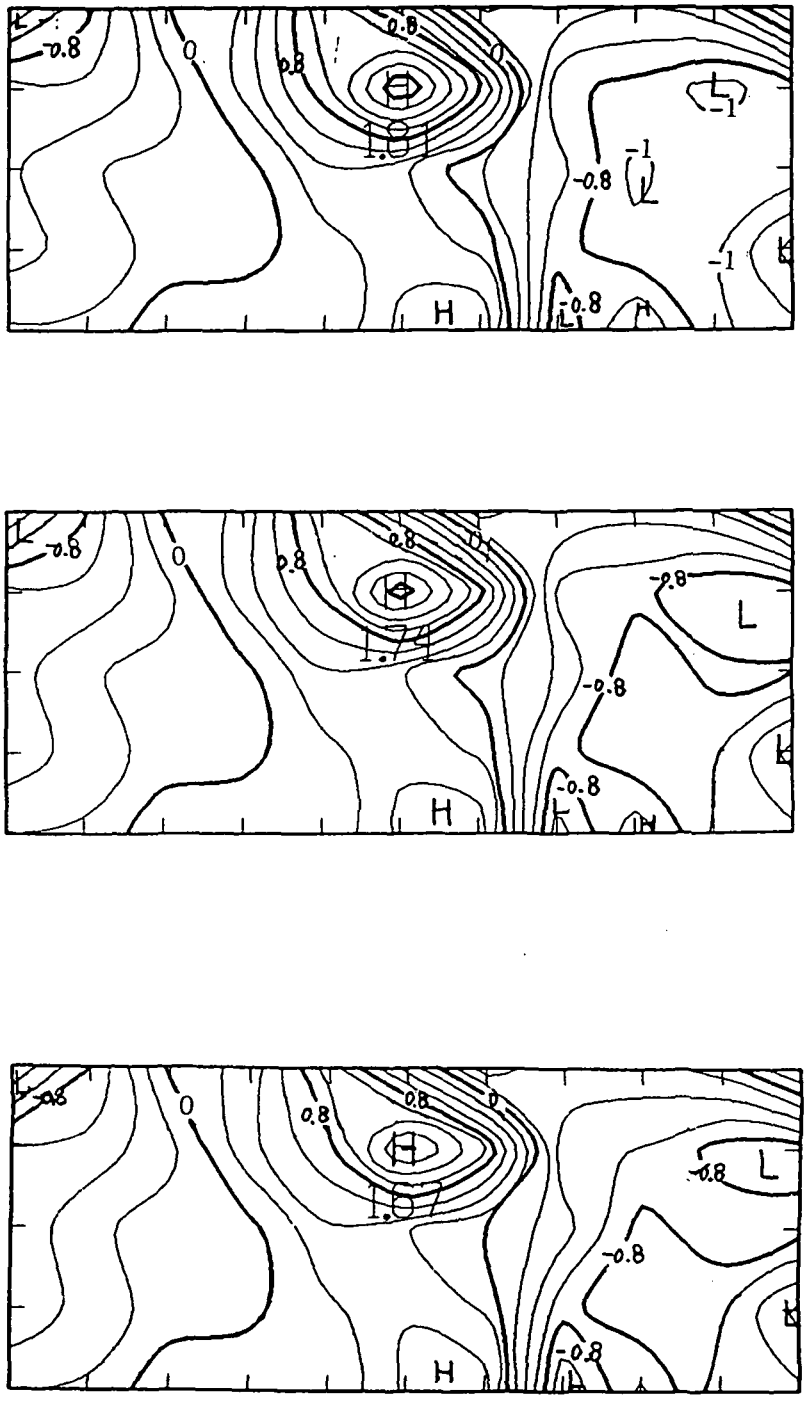


Fig. 11

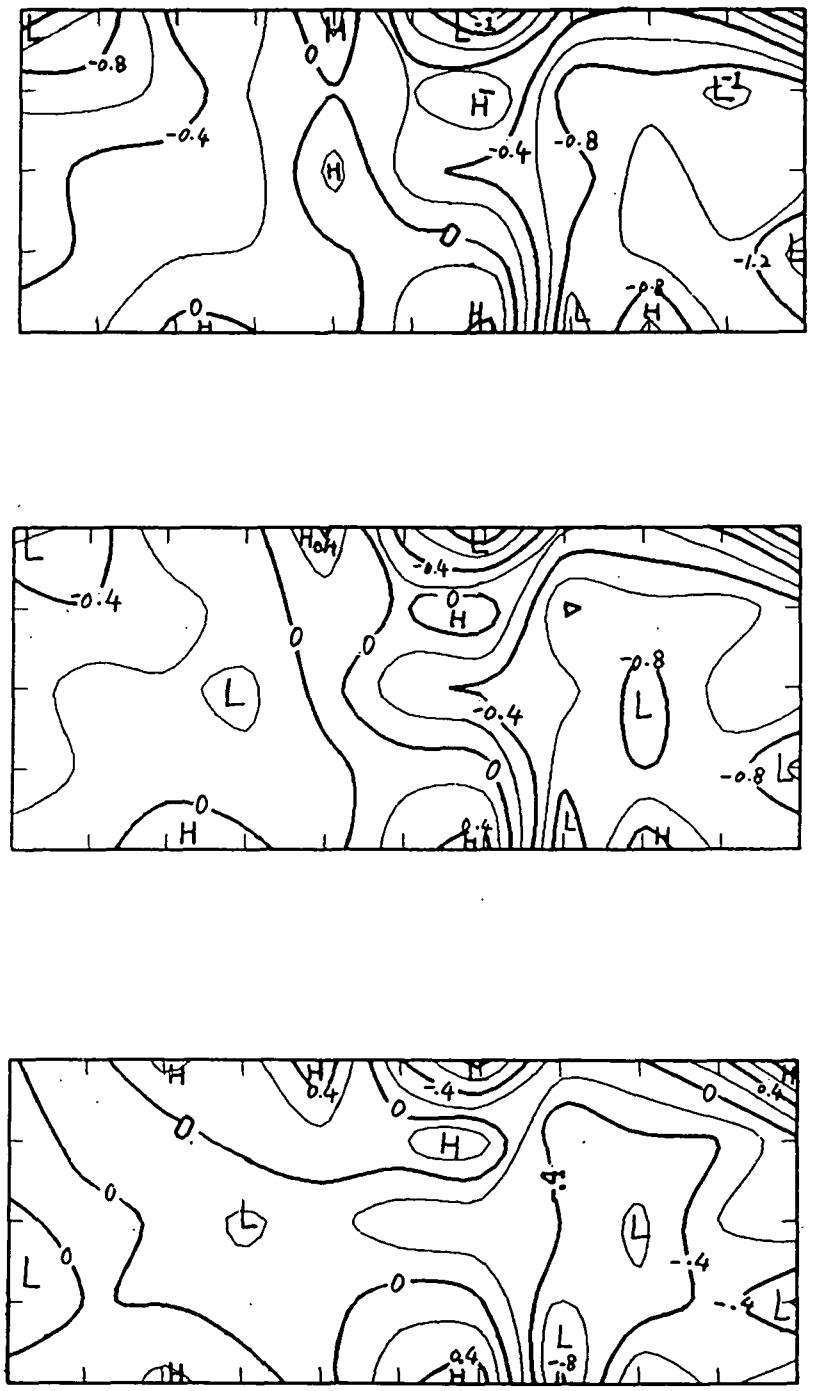


Fig. 12

REFERENCES

Barker, E., G.H. Haltiner, and Y.K. Sasaki, 1977: Three-dimensional initialization using variational analysis, **Proc. 3rd Conf. on Num. Wea. Pred., American Meteor. Soc.**, Omaha, Neb.

Baxter, T.L., and E.S. Goerss, 1981: Variational high-resoltuion metoeorlogical analysis, Final Report NASA Contract NAS5-26206.

Blackadar, A.K., and H. Tennekes, 1968: Asymptotic similarity in neutral barotropic atmospheric boundary layers. **J. Atmos. Sci., 25,** 1015-1020.

Brown, R.A., and W.T. Liu, 1982: An operational large-scale marine planetary boundary layer model. **J. Appl. Meteor., 21,** 261-269.

_____, V.J. Cardone, T. Guymer, J. Hawkins, J.E. Overland, W.J. Pierson, S. Peteherych, J.C. Wilkerson, P.M. Woiceshyn, and M. Wurtele, 1982: Surface wind analyses for SEASAT. **J. Geophys. Res., 8,** 3355-3364.

Businger, J.A., **et al.**, 1971: Flux-profile relationships in the atmospheric surface layer. **J. Atmos. Sci., 28,** 181-189.

Dome, G.J., A.K. Fung, and R.K. Moore, 1977: An empirical model for ocean radar backscatter and its application in inversion routine to estimate winds speed and direction effects. Paper presented at Proceedings URSI Commission F., La Baule, France, April 27 to May 6, 1977.

Garratt, J.R., 1977: Review of drag coefficients over oceans and continents. **Mon. Wea. Rev., 105,** 915-929.

Gray, W.M., 1972: A diagnostic study of the planetary boundary layer over the oceans. Atmos. Sci. Paper No. 179, Colorado State University, 95 pp.

Haltiner, G.H., and R. Williams, 1980: **Numerical Weather Prediction and Dynamic Meteorology**, 2nd Ed., John Wiley & Sons, 477 pp.

Jones, W.L., F.J. Wentz, and L.C. Schroeder, 1978: Algorithm for inferring winds stress from SEASAT-A. **AIAA J. Spacecraft Rockets, 15,** 368-374.

-----, L.C. Schroeder, D.H. Boggs, E.M. Bracalente, R.A. Brown, G.J. Dome, W.J. Pierson, and F.J., Wentz, 1982: The SEASAT-A satellite scatterometer: The geophysical evaluation of remotely sensed wind vectors over the ocean. **J. Geophys. Res.,87,** 3297-3317.

Moore, R.K., and A.K. Fung, 1979: Radar determination of winds at sea, **Proc. IEEE,67,** 1504-1521.

Pierson, W.J., V.J. Cardone, and E.A. Greenwood, 1974: The applications of SEASAT-A to meteorology. Tech. Report, City University of New York.

Sasaki, Y.K., 1958: An objective analysis based on the variational method, J. Meteor. Soc. Japan, **36.** 77-78.

_____, 1969: Proposed inclusion of time variation terms in numerical variatioanl objective analysis, J. Meteor. Soc., Japan, **47**, 115-124.

Schroeder, L.C., D.H. Boggs, G. Dome, I.M. Halberstam, W.L. Jones, W.J. Pierson, and F.J. Wentz, 1982: The relationship between wind vector and normalized radar cross section used to derive SEASAT-A satellite scatterometer winds. **J. Geophys. Res., 87**, 3318-3336.

Tennekes, H., 1973: Similarity laws and scale relations in planetary boundary layers. **Workshop on Micrometeorology**, A.M.S., Boston, 177-216.

Wright, J.W., 1966: Backscattering from capillary waves with application to sea clutter. **IEEE Trans. Antennas Propagat., AP-14**, 749-754.